

## Article

# Continuous Extraction and Continuous Backfill Mining Method Using Carbon Dioxide Mineralized Filling Body to Preserve Shallow Water in Northwest China

Yujun Xu <sup>1</sup> , Liqiang Ma <sup>1,2,\*</sup>, Ichhuy NGO <sup>1</sup> and Jiangtao Zhai <sup>1</sup>

<sup>1</sup> Key Laboratory of Deep Coal Resources Mining, China University of Mining and Technology, Ministry of Education, Xuzhou 221116, China; xyj@cumt.edu.cn (Y.X.); ngoichhuy@cumt.edu.cn (I.N.); tb21020005b3ld@cumt.edu.cn (J.Z.)

<sup>2</sup> School of Energy, Xi'an University of Science and Technology, Xi'an 710054, China

\* Correspondence: tb20020008b1@cumt.edu.cn; Tel.: +86-198-1625-2755

**Abstract:** The exploitation and utilization of coal resources are not only prone to causing water table lowering, but also produce a large amount of CO<sub>2</sub> and coal-based solid waste. A scientific concept that employs the CO<sub>2</sub> and solid wastes to develop filling bodies and inject them into the mined-out area, to sequester CO<sub>2</sub> and mitigate the overburden migration and thus preserve the overlying aquifer, is proposed. Continuous extraction and continuous backfill (CECB) mining was selected as the mining method to meet the aforementioned objectives. Additionally, carbon dioxide mineralized filling body (CMFB) under ambient temperature and pressure was developed, with fly ash as aggregate, and CO<sub>2</sub> gas, silicate additives and cement as accessories. The uniaxial compressive strength (UCS) and tensile strength of CMFB with various curing times and fly ash contents were tested indoors. A physical analogue simulation and FLAC<sup>3D</sup> numerical calculation were then successively implemented on the premise of determining a similar material ratio of CMFB in analogue simulation and calibrating the parameters of the CMFB in numerical simulation. The deformation of aquifer and water level lowering while using CECB and CMFB with various proportion of fly ash were obtained. When using the CMFB with 75% fly ash content and 28 d curing time, the maximum values of vertical displacement, horizontal displacement, inclination, horizontal deformation and curvature of aquiclude were 26 mm, 6.5 mm, 0.12 mm/m, 0.08 mm/m and 0.0015 mm/m<sup>2</sup>, respectively, and the water table decreased 0.47 m. The results show that the CMFB with 75% fly ash is the most appropriate ratio to realize water preservation mining, CO<sub>2</sub> sequestration and harmless treatment of solid wastes, contributing to the green and sustainable development of coal areas.

**Keywords:** continuous extraction and continuous backfill (CECB); water preservation coal mining; carbon dioxide mineralized filling body (CMFB); aquifer deformation; shallow water level lowering



**Citation:** Xu, Y.; Ma, L.; NGO, I.; Zhai, J. Continuous Extraction and Continuous Backfill Mining Method Using Carbon Dioxide Mineralized Filling Body to Preserve Shallow Water in Northwest China. *Energies* **2022**, *15*, 3614. <https://doi.org/10.3390/en15103614>

Academic Editor: Sergey Zhironkin

Received: 6 April 2022

Accepted: 12 May 2022

Published: 15 May 2022

**Publisher's Note:** MDPI stays neutral with regard to jurisdictional claims in published maps and institutional affiliations.



**Copyright:** © 2022 by the authors. Licensee MDPI, Basel, Switzerland. This article is an open access article distributed under the terms and conditions of the Creative Commons Attribution (CC BY) license (<https://creativecommons.org/licenses/by/4.0/>).

## 1. Introduction

China's coal reserves are mainly distributed in northwest regions, among which those in Shanxi, Shaanxi, Inner Mongolia and Xinjiang are the most abundant and account for nearly 70% of China's total coal resources [1]. With the depletion of coal resources in east China, the focus of coal mining has gradually shifted to northwest China with an arid and semi-arid climate. Northwest areas are already the main coal producing areas in China, where the proved reserves make up more than two-thirds of the country's total [2–4].

However, the main coal producing areas in northwest China feature a dry climate, sparse vegetation, land desertification and water shortage. The water resources account for only 3.9% of the total water resources [5]. The Quaternary Salawusu formation aquifer is the only shallow aquifer with the significance of being a residential and ecological water supply [6–8]. Large-scale and high-intensity coal mining has resulted in the movement and destruction of the overburden, and the fractures in the overlying layers are prone to

occur. If the fissures act as a hydraulic exchange zone between the shallow aquifer and the goaf, a large amount of water in the aquifer will flow into the mined-out area, breaking the original supplement, runoff and discharge balance state of the aquifer, and thus lead to sharp water table lowering and large-range water resource loss [9,10]. Taking the water level statistics of the Yu-Shen coal area in Shaanxi Province as an example, an area where the water level drop is greater than 8 m and has exceeded 650 km<sup>2</sup>, more than 70% is directly induced by high-intensity mining, which directly exacerbates the deterioration of the regional ecological environment [11]. In-depth research on water resource preservation and conservation in the mining areas has been conducted locally and abroad. Foreign experts analyzed the relationship between the mining-induced groundwater flow and the overlying strata migration and fracture development [12–14]. They studied the impact law of longwall mining on the water level of the overlying aquifer and the surrounding water environment, and evaluated the potential impact of mining on the surface and groundwater [15–18]. Additionally, the mining method was optimized according to the measured data of mining-induced groundwater level fluctuation obtained by the groundwater monitoring network [19–22]. The surface water and shallow aquifer were therefore protected from interference or damage, contributing to the realization of the sustainable and coordinative development of coal resources and shallow water resources [23–25]. Aiming at the problem of shallow surface water leakage during the process of coal mining in the Yu-Shen mining area, domestic scholars put forward the concept of water-preserving mining, and expounded its scientific connotation systematically [26]. They studied the stability of a water-resisting layer beneath the shallow water, and analyzed the relationship between the water table lowering and mining magnitude [27–29]. Water conservation mining methods, such as backfill mining, harmonic mining, partial mining, curtain grouting, overburden bed separation grouting and coal mine underground reservoir construction, have been proposed and put into implementation [30], the first of which is currently the most effective one for water preservation during coal extraction. Backfill mining includes longwall and shortwall backfill, and the former is confronted with the problems of insufficient filling time and filling space, and mutual impact and restriction between extraction and filling [31–35]. In view of the aforementioned problems, a CECB water preservation mining method which can realize the parallel and coordinated operation of mining and filling was proposed, contributing to mitigating the overburden migration and thus achieving extracting coal body beneath the shallow water [36–42].

On the other hand, the annual output of fly ash in 2018 in China exceeded 550 million tons, and the total storage volume was more than 3 billion tons [43]. Large quantities of fly ash produced by the combustion of coal in power plants have been causing air and soil pollution [44,45]. Harmless and large-scale treatment of fly ash is therefore necessary and urgent. Meanwhile, CO<sub>2</sub> emissions from coal consumption account for 72% and 28% of Chinese and global CO<sub>2</sub> emissions, respectively. The combustion of 1 ton of coal produces 2.4 tons of CO<sub>2</sub> [46]. In 2018, China's coal combustion emitted around 7.2 billion tons of CO<sub>2</sub> and it strives to achieve a carbon peak by 2030 and be carbon neutral by 2060 [47–50]. In this context, carbon sequestration has attracted the attention of the Chinese government and emphasis has been put on it. However, the total amount of carbon sequestration is only about 300,000 t/a, which is not enough to provide effective support for this goal [51]. In order to effectively cope with the continuous increase in CO<sub>2</sub> emissions and fly ash, sequestering CO<sub>2</sub> to fly ash and developing CO<sub>2</sub> mineralized filling body (CMFB) is one of the most ideal and appropriate options [52]. CMFB is employed and injected into the mined-out area of mining roadways (MRs) of the CECB mining method to realize CO<sub>2</sub> sequestration. In the meantime, solid CMFB replaces coal body to support the roof and mitigate the migration of the overburden and water-resisting layer, which can help to preserve the valuable shallow water resources and achieve green and sustainable development of coal areas. However, the mechanical properties of CMFB with various material ratios, and the influence of CMFBs on mining-induced aquifuge stability, which is of great importance for shallow water preservation, are not clear. The control mechanism of

CMFBs on the shallow water level while using the CECB mining method requires further study. Further study to develop CMFB with different material ratios to not only sequester  $\text{CO}_2$  but preserve and conserve the shallow water level, and thus protect and maintain the surface ecological environment, is necessary.

In view of the aforementioned problems, we carry out a prospective study on the development and application of CMFB at ambient pressure and temperature, with fly ash as aggregate and silicate additives, cement and  $\text{CO}_2$  gas as accessories. The indoor mechanical parameter test of the CMFB with different curing times and material ratios is carried out. Based on the stress–strain curve of the testing results, the proportion of analogue materials of CMFB is optimized and determined, and the physical similarity simulation of overburden movement while using the CECB mining method and CMFB is implemented. Additionally, the CMFB strain-softening parameters in the numerical simulation are calibrated systematically, and the FLAC<sup>3D</sup> numerical calculation model is then constructed to simulate the aquiclude movement corresponding to CMFB with different fly ash contents while using the CECB mining method. Subsequently, the fluid–solid coupling module is employed to reveal the influence mechanism of different material ratios of CMFB on the variation law of the shallow aquifer water level. This paper proposes a concept that employs the CECB water preservation coal mining method to sequester  $\text{CO}_2$  and replace the coal body to support the roof, contributing not only to the harmless treatment of fly ash, but also the achievement of shallow water preservation mining. The research results can provide a theoretical reference and guidance for the realization of  $\text{CO}_2$  mineralized filling in mines in the future, which is conducive to green and sustainable mining.

## 2. CECB Mining Method to Sequester $\text{CO}_2$ and Preserve Shallow Water

The confined room is necessary for the  $\text{CO}_2$  mineralization process and CECB mining is an ideal mining method to provide a closed space for CMFB since the MRs features good airtightness and flexible and adjustable dimensions. The  $\text{CO}_2$  can be mineralized with the solid waste in the long run and water preservation can be realized by optimizing the material ratio of the CMFB and the dimensions of MRs.

Prior to CECB mining, the mining panel is divided into many MRs along two sides of the headgate, and the MRs are then allocated to different mining phases (generally 3–5). The three-dimensional sketch map of the MR arrangement of the CECB method is shown in Figure 1. The schematic map of the mining processes of the CECB method is shown in Figure 2.

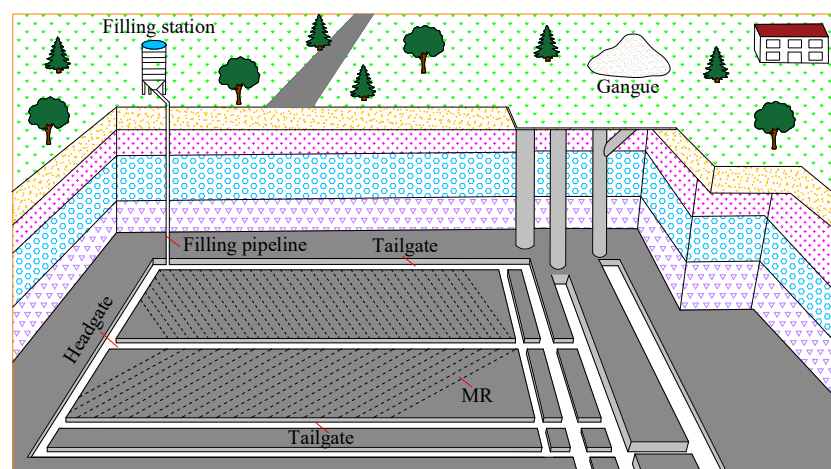


**Figure 1.** Three-dimensional sketch map of the MR arrangement of the CECB mining method.

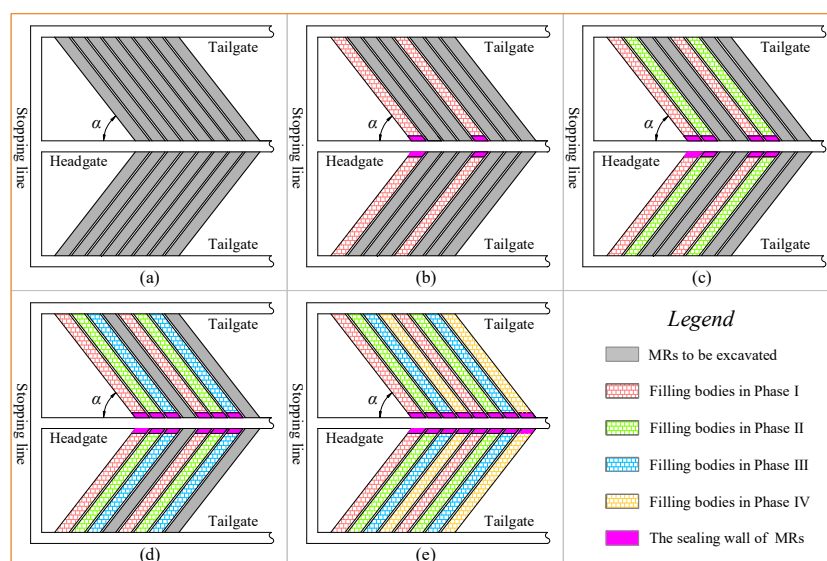


**Figure 2.** Schematic map of the processes of CECB. (a) The arrangement of MRs; (b) MRs of phase I have been excavated and filled; (c) MRs of phase II have been excavated and filled; (d) MRs of phase III have been excavated and filled; (e) MRs of phase IV have been excavated and filled. Reprinted with permission from ref. [32]. Copyright 2019 MDPI.

In order to mitigate the mining disturbance and thus to make the CMFB conducive to being injected, the length of the MR is generally less than 150 m while the width varies from 4.0 m to 7.0 m. The angle  $\alpha$  between the MR and the headgate usually ranges from 40 to 60°. Skip extraction enables the roof of each mined-out MR to be supported by the coal body or the CMFB which has reached the designed strength. Hence, the drastic overburden deformation caused by insufficient longwall filling time can be averted. This method avoids the problem of uncoordinated operations between mining and filling during the longwall filling process. In addition, skip mining and filling make it feasible for the CMFB to stay in the three-dimensional stress state, which can increase the support strength of the filling body before it reaches the final strength. Both sides of the MRs, having been extracted, are always coal body or filling body that have reached the designed strength, which is conducive to controlling the migration and deformation of the overlying strata. For the purpose of effectively mitigating the movement of the overlying layers and avoiding the instability of the aquifuge, each MR will be sealed by a sealing wall and backfilled immediately after it is extracted. The MRs in the second phase will be extracted and backfilled after all MRs in the first phase are mined and backfilled. Finally, coal body in the mining panel is completely substituted by the CMFB to support the roof and preserve the shallow water. The CO<sub>2</sub> sequestration and coal extraction under shallow water bodies can be realized.

### 3. Development of the Carbon Dioxide Mineralized Filling Body

#### 3.1. Specimen Preparation

The filling material is composed of aggregate and auxiliary materials, in which the aggregate plays the main bearing role as the main structure, and the auxiliary materials assume the roles of bonding, reinforcement and rapid setting. Low-calcium fly ash was selected as the aggregate, and CO<sub>2</sub> gas, silicate additives and cement were used as accessories to develop the CMFB with high content fly ash at ambient temperature and pressure. The grade F fly ash used in this study is from a power plant in Yuncheng City, Shanxi Province. OPC cement is from the local cement plant of Datun Town. Silicate additives were purchased online from Ningbo City, Zhejiang Province. The gas tank containing compressed CO<sub>2</sub> gas was bought from the local city.

The strength properties of the CMFB samples are highly dependent on the water–solid ratio. This research mainly studies the influence of the various ratios of the low-calcium fly ash to the cement on the uniaxial compressive strength (UCS) and tensile strength of CMFB, with the silicate additives and the concentration and flux of CO<sub>2</sub> being invariant. Therefore, a variable-controlling method was adopted to fix the water concentration at 30% of the total material, i.e., the water–solid ratio was set to 3:7. The test scheme is divided into 4 groups, namely FA55, FA65, FA75 and FA85, which denote the ratios of the fly ash to the total of the fly ash and the cement which are 55%, 65%, 75% and 85%, respectively. Each material ratio (the content of fly ash) includes two groups for the purpose of compressive and tensile tests. The curing times of each group are 3 d, 7 d, 14 d and 28 d, respectively. There are three specimens prepared for each setting time and each material ratio and each testing purpose, and the required number of compressive specimens and tensile specimens is  $4 \times 4 \times 3 \times 2 = 96$  specimens. The detailed scheme is listed in Table 1.

**Table 1.** The schemes of material ratios of CMFB.

Scheme	Solid Mass Percentage (70 wt%)		FA *:CM * Ratio	Liquid Mass Percentage (30 wt%)		CO <sub>2</sub>	Curing Time
	Fly Ash	Cement		Silicate Additives	Water		
FA55	55	45	11:9	10%	90 wt%	20 min	3/7/14/28
FA65	65	35	13:7	10%	90 wt%	20 min	3/7/14/28
FA75	75	25	15:5	10%	90 wt%	20 min	3/7/14/28
FA85	85	15	17:3	10%	90 wt%	20 min	3/7/14/28

\* FA refers to the fly ash and CM denotes the cement.

The mortar samples were prepared according to the standard regulated by the state (GBT17671-1999), and the main process of the sample preparation is shown in Figure 3.

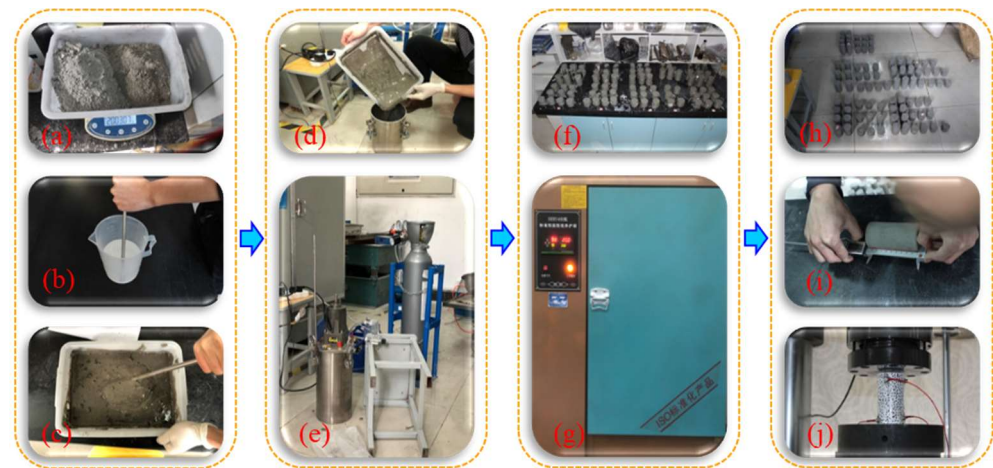


**Figure 3.** The process of CMFB specimen preparation and the mechanical tests.

① Weighing the fly ash and cement and mixing them evenly (Figure 3a). ② Weighing the particles of the silicate additives and putting them into a container to stir and melt (Figure 3b). ③ Mixing the dissolved silicate additive solution with evenly stirred fly ash and cement, and stirring until a uniform paste was obtained (Figure 3c). ④ Pouring the paste into the reactor with an automatic mixer, and stirring while introducing CO<sub>2</sub> gas for 20 min (Figure 3d,e). ⑤ Pouring the filling slurry into the standard molds made of a Jacqueline tube with dimensions of  $\varphi 50 \text{ mm} \times 100 \text{ mm}$  and  $\varphi 50 \text{ mm} \times 50 \text{ mm}$ , and shaking slightly to remove the incompletely reacted CO<sub>2</sub> bubbles. The noteworthy detail is that the bottoms of the molds were sealed with tape, and the bottoms and the tube wall of the molds were coated with waste oil to prevent the slurry from sticking to the mold (Figure 3f). ⑥ Taking out the samples from the molds after 12 h to 15 h after they were

poured, and putting them in the SHBY-40B standard curing box with constant temperature and humidity. The humidity is controlled at around 98%, with the curing temperature being  $20 \pm 2$  °C, and the samples were cured for 3, 7, 14 and 28 days, respectively (Figure 3g). ⑦ The dimensions of the CMFB samples after the curing expiration was calibrated to make it a standard cylindrical filling body test piece that meets the dimension requirements of the mechanical test. Meanwhile, the upper and lower surfaces of the samples were polished smooth, and then the uniaxial compression tests and Brazilian splitting tests were implemented in the laboratory (Figure 3h–j).

The schematic diagram of CO<sub>2</sub> gas mixing with fresh slurry is shown in Figure 4.

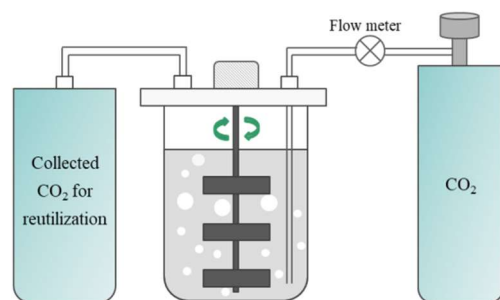


**Figure 4.** The chemical reaction between CMFB slurry and CO<sub>2</sub> is carried out under stirring.

### 3.2. Testing Results

#### 3.2.1. Uniaxial Compressive Strength (UCS)

The UCS is particularly significant to improving the surrounding rock stress environment and evaluating the mechanical stability of the overlying strata. The WAW-1000D electro-hydraulic servo motor test system, with maximum load of 50 kN, was employed as the loading equipment in the experiment to test the UCS of the CMFB with various curing times and fly ash proportions. The displacement-controlled loading mode was adopted during the tests. Firstly, the fixed CMFB specimen was preloaded at a constant loading speed of 3 mm/min, and the target value was 0.05 kN, so that the filling body was in contact with the loading equipment. Then the force and displacement monitored on the computer was cleared, and the constant loading speed was adjusted to 0.3 mm/min and the target value was reset to 10 mm to conduct the UCS test. All tests were repeated 3 times to eliminate errors and the average value of UCS of each curing time and fly ash content was obtained.

The UCS variation laws of CMFBs with various curing times and fly ash contents are shown in Figure 5a,b, respectively. Some of the failure specimens after UCS test are illustrated in Figure 5c. According to the previous experience of filling body development without CO<sub>2</sub> [8], the UCS will decrease with increasing fly ash content, due to the fact that a drop in the latter means a decrease in hydration products. To the contrary, the UCS of CMFB samples increases first and then decreases with the rising proportion of the fly ash, reaching the maximum at 75%, and then decreases, showing almost the opposite trend to that of the filling body without CO<sub>2</sub>. It is worth noting that when the fly ash content is 95%, the UCS of CMFB is too small to withstand preloading. The UCS of CMFB with 85% fly ash is 1.982, 2.356, 3.832 and 4.162 MPa, respectively, corresponding to curing times of 3, 7, 14 and 28 days. The UCS of CMFB with 85% fly ash is not only lower than those with 75% fly ash but also less than those with 65% in each curing time. Therefore, the addition of CO<sub>2</sub> and silicate additives exerts a significant impact on the UCS of CMFB. By analyzing the chemical reaction of different materials, we hold the view that the CO<sub>2</sub> accelerates the initial hydration of CMFB slurry and makes it able to form silica gel. In other words, the accelerated hydration and silica gel replaced the cementation identity of cement, and thus increased the UCS of CMFB.

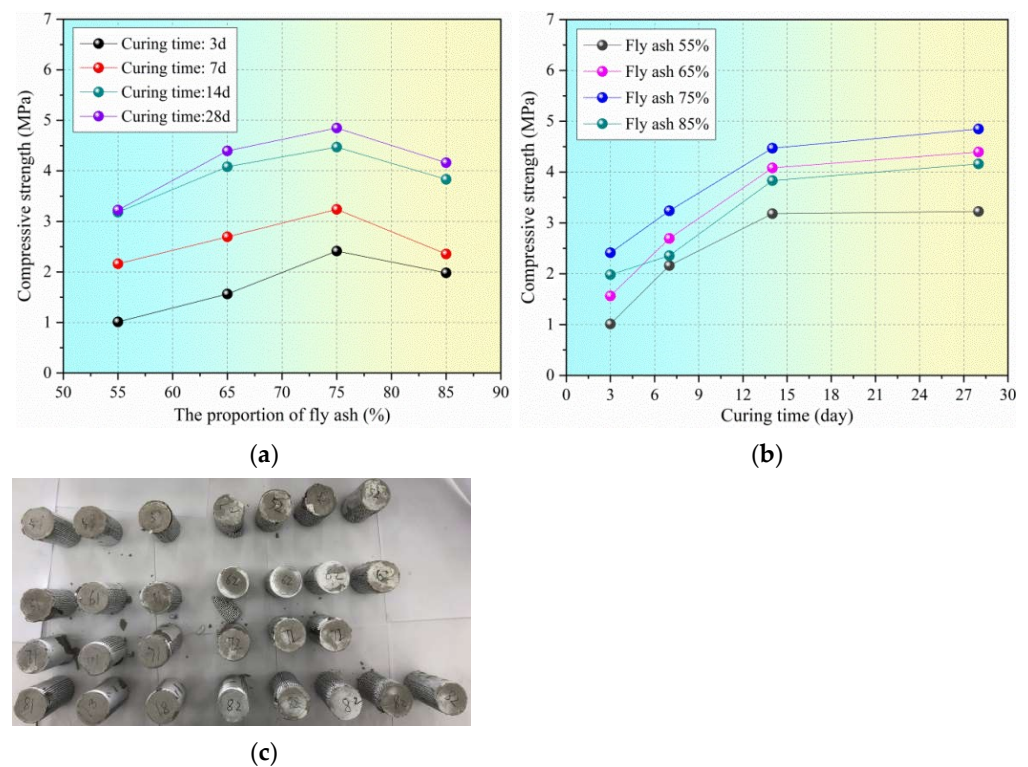


**Figure 5.** The UCS of CMFB with various fly ash contents and curing times. (a) Various fly ash contents; (b) various curing times; (c) some damaged specimens after the UCS test.

As Figure 5b shows, the UCS of CMFB rises with the growing setting time. The ascending curing time means more hydration, which implies more hydrates bind the particles together, and the occlusal friction between the particles leads to the increase in UCS. Taking the UCS of CMFB with 55% fly ash, for instance, the UCS is 1.012, 2.162, 3.181 and 3.224 MPa, corresponding to curing times of 3, 7, 14 and 28 d, respectively. The UCS grows sharply from 3 to 14 d curing time while it increases slightly from 14 to 28 d, which means the hydration after 14 d starts declining drastically.

### 3.2.2. Tensile Strength

During the field investigation of backfill mining face, it is found that many filling bodies suffer from instability due to the insufficient tensile strength and the incapability of resisting tensile deformation. Both the compression and bending failure of filling bodies are caused by tensile strain or shear strain exceeding the ultimate bearing capacity. It is therefore necessary to study the tensile strength of the filling body. By analyzing the mechanical properties from the indoor tensile test, the support quality of the filling body to the roof can be improved, and thus the stability of the overlying aquifer and shallow water level can be maintained.

The Brazilian splitting method, a popular indirect measurement method, was employed for the indoor tensile strength test of the CMFB. The CMFB specimen was damaged along the radial direction under the load, rather than the splitting of the whole specimen. In addition, the surface roughness of most specimens means the linear loading cannot be guaranteed to be uniform, resulting in large dispersion of the measured data. Therefore, extra specimens were added to eliminate the problem of large dispersion of tensile strength data. The relationship between the tensile strength and the curing time and the content of fly ash, as well as the failure conditions of the specimens after the Brazilian splitting test, are shown in Figure 6.

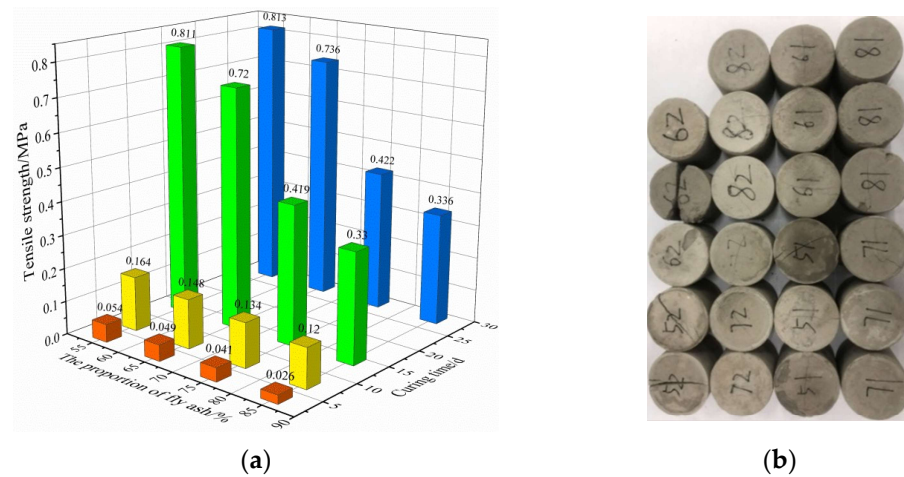


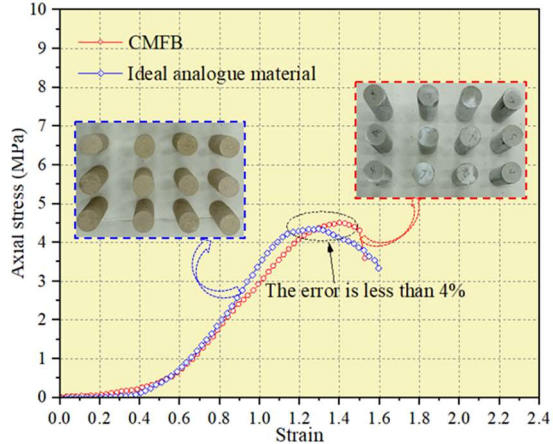
**Figure 6.** The tensile strength of CMFB and the physical map of specimens. (a) The tensile strength of CMFB with various curing times and fly ash contents; (b) the physical map of some specimens after the Brazilian splitting test.

**4. Deformation of the Overlying Strata and Aquifuge**

**4.1. Main Parameters of Analogue Simulation**

Based on the engineering and geological conditions of a coal mine in northwest China, a physical analogue model with dimensions of 2.5 × 0.2 × 1.24 m (length × width × height) was built in the laboratory in accordance with the principles of similarity theory. The geometric similarity ratio is 1:200. The model is divided into four mining phases, with 10 MRs in each mining phase. After all MRs in a mining phase are mined and backfilled, the MRs in the next phase start being extracted and filled until all MRs in the four mining phases are mined and filled. The dimensions of each MR are 6.0 × 2.6 m (width × height), and the filling rate is around 90% since the roof subsides before backfill.

Sand, calcium carbonate, gypsum, etc. were selected as raw materials to develop physical similarity materials of CMFB. The UCS stress–strain characteristics of similar materials with different material ratios were tested, and the stress–strain curves were compared with that of CMFB with 14 d curing time and 75% fly ash, so as to select the optimal material ratio of similar materials of CMFB for the physical similarity simulation. The test results of the stress–strain curves of the selected ideal similar material and the CMFB are shown in Figure 7, with the error being less than 4%. The material mixture ratio of strata and the CMFB in the analogue model is shown in Table 2.

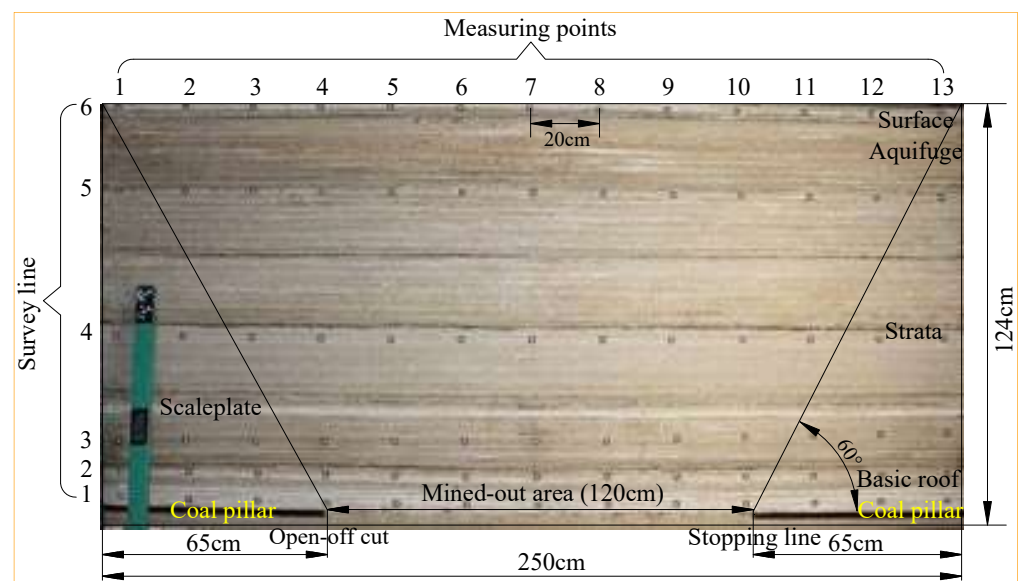


**Figure 7.** The stress–strain curves of the CMFB and its similar materials in analogue simulation.

**Table 2.** The material ratios of strata and CMFB in the physical analogue model.

No.	Lithology	Thickness (cm)	Water (kg)	Sand (kg)	Calcium Carbonate (kg)	Gypsum (kg)	Total (kg)	Remarks
1	Loess	4.0	1.67	13.64	0.68	0.68	16.67	Aquifer
2	Red clay	25.0	6.24	49.23	3.51	3.51	62.49	Aquifuge
3	Sandstone	16.6	8.96	69.11	5.76	80.63	164.46	
4	Sandy mudstone	31.5	18.95	149.32	10.66	10.66	189.59	
5	Medium sandstone	4.5	4.82	25.31	5.91	2.53	38.57	
6	Mudstone	21.0	15.41	121.41	8.67	8.67	154.16	Bedrock
7	Sandstone	3.0	2.5	18.76	1.88	1.88	25.02	
8	Fine sandstone	7.8	6.46	42.19	4.22	4.22	57.09	
9	Limestone	4.6	1.9	12.19	1.78	1.03	16.90	Roof
10	Coal seam	1.3	1.04	8.20	0.82	0.35	10.41	Coal
11	Bauxitic mudstone	4.7	1.04	8.33	0.52	0.52	10.41	Floor
12	CMFB	1.3	1.12	8.31	0.75	0.28	10.46	CMFB

After the analogue model was laid and dried for ten days, six survey lines were set in the front of the model to measure the deformation of the overlying layers and especially the aquifuge. Each survey line consists of 13 measuring points, and the distance between each measuring point is 0.2 m. The purpose of survey Line 1 is to monitor the deformation of the main roof, while Line 2 to Line 4 aim to measure the migration of the bedrock. Line 5 and Line 6 are arranged to monitor the deformation of the aquifuge and ground surface, respectively. The analogue model after all MRs are extracted and backfilled, as well as the arrangement of the measuring points, are shown in Figure 8.

**Figure 8.** Physical analogue model of CECB mining after all MRs are extracted and backfilled.

#### 4.2. Results of Analogue Simulation

The results indicate that there are no obvious fractures or cracks in the overlying strata and each stratum is still intact and undamaged after all MRs in the four mining phases are mined and backfilled, suggesting that the CECB method can effectively control the overlying strata migration and fracture development. During the experiment, the displacement of each measuring point was recorded by the Tianyuan 3D Photogrammetry System. The measured data were converted according to the geometric similarity ratio of 1:200. When all MRs were extracted and backfilled, the vertical displacement of 6 survey lines was monitored, as illustrated in Figure 9a. The dynamical deformation characteristics of the overlying aquiclude during four mining phases are shown in Figure 9b.

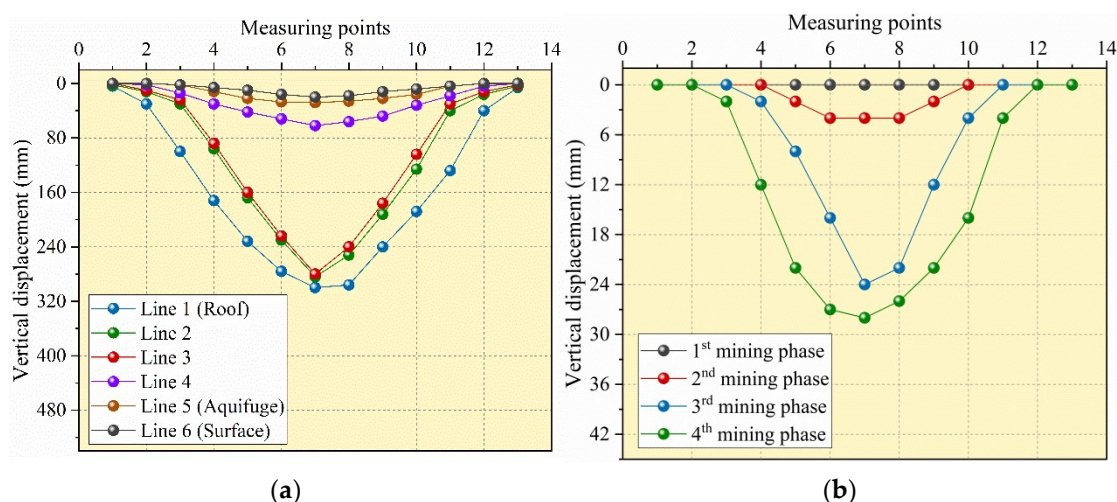


**Figure 9.** The deformation of the overburden and the aquifuge. (a) The vertical displacement of 6 survey lines after all MRs are extracted and backfilled; (b) the vertical deformation of the aquifuge during 4 mining phases.

The migration and displacement of the overlying strata in the last mining phase is of great significance for evaluating the roof-controlling effectiveness of the CECB mining. Therefore, the vertical displacement of the overlying strata in various positions was measured. As Figure 9a shows, after the MRs in the fourth mining phase were extracted and backfilled, the vertical displacement of the main roof and the lowest two strata of the bedrock, monitored by Line 1 to Line 3, is far more than that of the top stratum of the bedrock, the aquifuge and surface. The maximum vertical displacements of the six measuring lines are 300 mm, 284 mm, 280 mm, 62 mm, 28 mm and 20 mm, respectively. Moreover, the water-resisting layer measured by Line 5 was selected for separate analysis since its deformation is vital to prevent water flowing from its overlying aquifer, and thus realize shallow water preservation coal mining. It can be seen from Figure 9b that the vertical deformation of the aquifuge in the first stage remains stable and always equals 0, due to the long distance from the mining panel to the aquifuge and thus the low mining disturbance. During the first two mining stages, the vertical subsidence of the aquifuge rises slowly. By contrast, the vertical displacement of the water-resisting layer rises drastically from the 3rd to the 4th mining phase. After all MRs in the mining panel are extracted and filled, the maximum value of vertical displacement is 28 mm. Note that the value of horizontal displacement and horizontal deformation is too small to be detected by the Tianyuan 3D Photogrammetry System. The five indexes of aquifuge deformation will be further studied in Section 5.

## 5. Numerical Simulation of Aquiclude Deformation Using CECB and CMFB

### 5.1. Construction of the Numerical Simulation Model

Fast Lagrangian Analysis of Continua (FLAC<sup>3D</sup>), a three-dimensional finite difference program developed by ITASCA in the United States, is one of the most widely used pieces of numerical analogue software in underground mining and geological engineering. The physical similar simulation model only detects vertical displacement of the aquifuge while the horizontal displacement is too small to detect. In addition, only CMFB with 14 d curing time and 75% fly ash content was taken into consideration in the physical simulation, which cannot study the influence of CMFB with different material ratios on the migration and stability of the aquifuge. In order to supplement the undetected horizontal displacement and horizontal deformation of the water-resisting layer and verify the results of the physical analogue simulation, a FLAC<sup>3D</sup> numerical calculation model was established to simulate the deformation and water table lowering of the aquiclude using CECB mining and CMFB with 14 d curing time and various fly ash proportions, as shown in Figure 10. Based on

the engineering and geological conditions of a colliery which are the same as the physical analogue simulation, the adjacent strata with similar lithology are properly simplified and merged, and 12 strata were identified from bottom to top. With due consideration of the boundary effect and full mining, the dimensions of the model are determined to be 612 m  $\times$  558 m  $\times$  248 m (X  $\times$  Y  $\times$  Z). The deformation and velocity of the four boundaries of the numerical model located at the starting and ending point of the X and Y axis remain immobile. Meanwhile, the boundary at the starting point of the Z axis was fixed while the top surface was free without any restrictions.

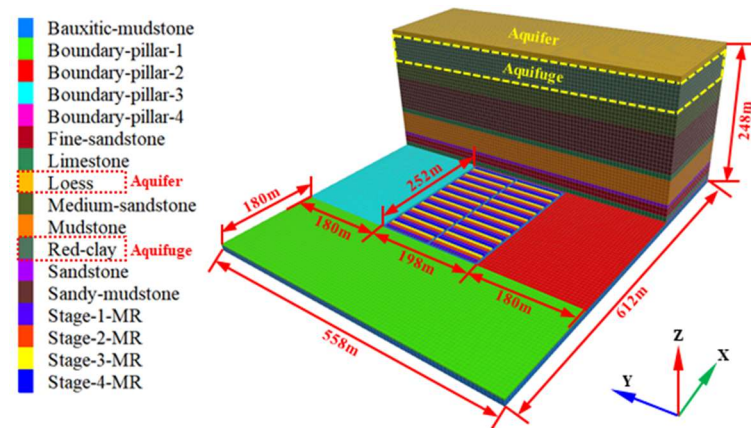


**Figure 10.** Numerical calculation model for simulating the aquifuge deformation under CECB.

The length of the four boundary coal pillars is 180 m. The mining panel whose dimensions are 240 m  $\times$  180 m (strike  $\times$  dip) is surrounded by a haulage roadway with width of 6 m. The height and width of the MR are 2.6 m and 6 m, respectively. The CECB mining area is divided into four phases, and a total of 80 MRs are distributed on both sides of the main transportation roadway. There are 20 MRs in each phase, and skip and interval mining are adopted on the same side along the main haulage roadway. After one MR is mined, the next one on the other side of the main haulage roadway is extracted immediately and the mined-out MR is backfilled simultaneously. The third MR, which is 24 m (four times of the MR width) away from the first MR in the X direction, is extracted in the same way as the first MR. When the MRs in the first phase is mined and backfilled, the MRs in the second phase start being extracted and filled until all MRs in the four phases are extracted.

A Mohr–Coulomb constitutive model was chosen for the coal seam and its overlying and underlying strata. Therefore, it was employed to conduct uniaxial compression simulation tests of rock from various strata, so as to determine the mechanical parameters of different strata. The mechanical parameters of each stratum in the model are adjusted continuously, until the simulation results show good consistency with the stress–strain curve obtained from the laboratory test. The mechanical property parameters of various strata are listed in Table 3.

### 5.2. Determination of the Simulation Parameters of CMFB

According to the research in Section 3, the UCS of the CMFB increases rapidly when the setting time varies from 3 d to 14 d, while it slows down from 14 d to 28 d curing time, indicating that its strength and mechanical properties tend to be stable. Similarly, it takes 3 days to extract the coal body of each MR and 1 day to backfill it. The distance between the MR being extracted and the MR that was backfilled 14 days ago is generally greater than 70 m, so the filling body in the MR before day 14 is essentially immune to the current mining. It only bears the static load generated by ground pressure, and its mechanical environment is inclined to remain unchanged. Therefore, CMFB with 14 d curing time was selected for further analysis.

**Table 3.** The mechanical parameters of strata and coal seam of the numerical model.

Strata	Bulk Modulus (GPa)	Shear Modulus (GPa)	Cohesion (MPa)	Friction Angle (°)	Tensile Strength (MPa)	Bulk Density (kN·m <sup>3</sup> )	Thickness (m)
Loess	-	-	-	-	-	14.7	8
Red clay	0.08	0.05	0.33	27	0.12	19.7	50
Medium sandstone	3.2	2.0	1.6	31	1.4	20.6	33.2
Sandy mudstone	2.8	1.7	1	22	1	19.7	63
Limestone	7.2	5.5	2	40	4.0	24.0	9
Mudstone	2.9	2.1	1.4	19	1.1	28.6	42
Sandstone	6.81	5.91	10.7	40.6	2.2	2540	6
Fine sandstone	3.8	2.6	1.6	31	1.4	20.6	15.6
Limestone	7.2	5.5	2	40	4.0	24.0	9.2
Coal	2.2	0.76	1	20	1	18.7	2.6
Bauxitic mudstone	4.2	2.8	1.4	34	1.4	28.6	9.4

Moreover, the Young's modulus of the backfill is a significant index reflecting its supporting capacity to the overburden and water-resisting layer. The filling body with large elastic modulus has better mechanical properties, which can effectively alleviate the deformation and fracture development of the overburden, so as to reduce the mining-induced impact on the shallow aquifer. Conversely, the backfill with small elastic modulus has greater deformation under the same load than that of the larger one, leading to the increasing subsidence of overlying layers. The water-flowing fractures will therefore be well developed, which may form a water-conducting channel between the mined-out area and the overlying aquifer and trigger a mine water inrush disaster. According to the UCS test results of CMFB from the laboratory, the proportion of fly ash has a great influence on the elastic modulus of the backfill, while the Poisson's ratio is nearly unchanged and remains at 0.18 on average. The elastic modulus can be obtained by analyzing the slope of the stress–strain curve in the elastic deformation stage:

$$E_f = \frac{\sigma_b - \sigma_a}{\varepsilon_b - \varepsilon_a}, \quad (1)$$

where  $E_f$  is the elastic modulus of CMFB;  $\sigma_a$  and  $\sigma_b$  represent the stress of the starting and terminal point of the elastic deformation stage, respectively;  $\varepsilon_a$  and  $\varepsilon_b$  denote the strain of the origin and the end of the elastic deformation stage, respectively.

The bulk modulus and shear modulus can be calculated by:

$$K_f = \frac{E_f}{3(1-2\mu)}, G_f = \frac{E_f}{2(1+\mu)}, \quad (2)$$

where  $K_f$  is the bulk modulus,  $G_f$  is the shear modulus and  $\mu$  is the Poisson's ratio.

Table 4 lists the mechanical property parameters such as elastic modulus, bulk modulus and shear modulus of CMFB with different fly ash contents after being cured for 14 days.

**Table 4.** The physical and mechanical parameters of CMFB with 14 d curing time and various fly ash contents.

Proportion of Fly Ash (%)	Young's Modulus (GPa)	Bulk Modulus (GPa)	Shear Modulus (GPa)
FA55	0.4	0.21	0.17
FA 65	0.6	0.31	0.25
FA 75	1.0	0.52	0.42
FA 85	0.5	0.26	0.21

The strain-softening constitutive model was employed for CMFB. The cohesion, friction, dilation and tensile strength may soften after the beginning of plastic yield, while these properties are assumed to remain unchanged in the Mohr–Coulomb model. The strain-softening behavior of cohesion, friction angle and dilation based on plastic shear strain and plastic tensile strain were given in the form of specified table values, assuming that the two parameters in the table code are consecutive. The table values of these parameters were defined by the authors and they were obtained by back-analysis of the postfailure behavior of the CMFB.

Taking the CMFB with 14 d curing time and 75% fly ash content as an example, the stress–strain curves of the UCS test from the laboratory test and the numerical simulation, as well as the failure form of the CMFB specimen and the maximum shear strain of the numerical simulation model, were compared and analyzed to systematically calibrate the aforementioned parameters of the strain-softening constitutive model. The calibration results are shown in Figure 11.

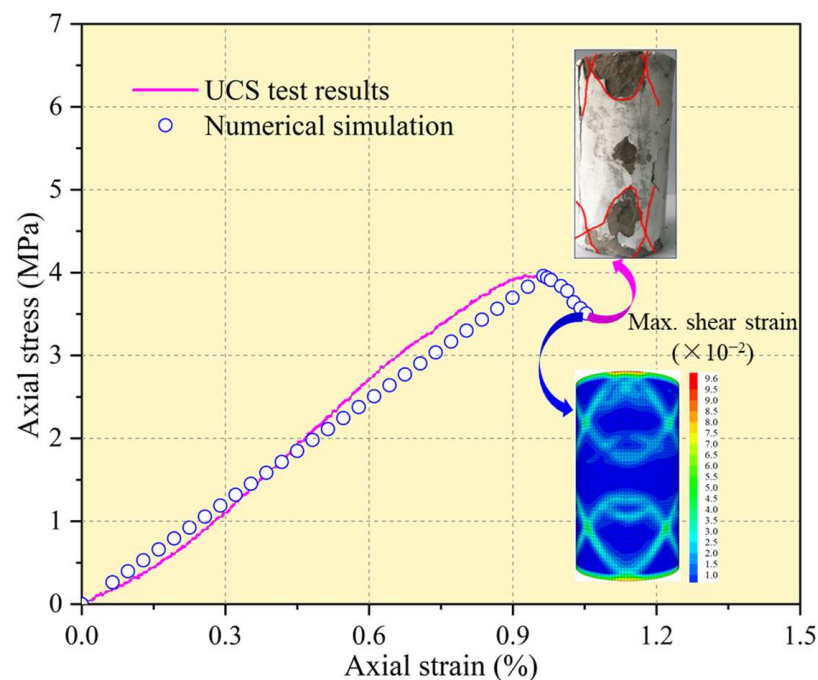


**Figure 11.** The stress–strain curves and failure model of CMFB from the laboratory UCS test and the numerical simulation.

This simulation considers that the cohesion and friction of CMFB decrease with the growing plastic shear strain, for the purpose of optimizing the numerical calculation steps. Their values are the residual value when the plastic shear strain is 0.01. The numerical results of the stress–strain curve and failure mode of the specimen were in good agreement with that of the indoor test results. In the numerical model, the maximum shear strain of the specimen shows an inclined and cross failure mode, which is consistent with that from the laboratory test. The parameters of the strain-softening model of the CMFB with various fly ash contents were calibrated and determined by the same means for the next study.

### 5.3. Mining-Induced Deformation of the Water-Resisting Layer

According to the calibrated strain-softening mechanical parameters of the CMFB, the numerical calculation of the movement of the water-resisting layer while using CECB mining and CMFB was carried out. After all MRs in the mining panel were extracted and backfilled and the maximum unbalance force was less than  $10^{-5}$  kN, the numerical calculation process ended. The bottom of the aquiclude was sliced, with the normal vector parallel to the Z axis. Subsequently, the postprocessing software Tecplot was employed to extract the vertical and horizontal displacement values of the aquifuge in the section, and

the extracted data were imported to another postprocessor Surfer. The Kriging interpolation method was adopted to draw the contour of the vertical displacement and the horizontal displacement of the aquiclude while using the CECB water-preserving mining. Then, the differential function built into the Surfer software was utilized and the contour map of the inclination, curvature and horizontal deformation of the aquifuge were derived, by executing the first-order and second-order differential functions embedded in the software. Figure 12 shows the contour map of the five deformation indicators of the overlying aquifuge while injecting the CMFB with a 75% fly ash proportion into the mined-out MRs.

Both the positive and negative deformation values can reflect the migration and damage degree of the rock stratum, so only the absolute value was analyzed. As Figure 12 shows, under the conditions of injecting the CMFB, with the proportion of fly ash being 75%, into the mined-out MRs in the CECB mining panel, the maximum values of vertical displacement, horizontal displacement, inclination, horizontal deformation and curvature of the overlying aquifuge are 26 mm, 6.5 mm, 0.12 mm/m, the 0.08 mm/m and 0.0015 mm/m<sup>2</sup>, respectively.

The maximum vertical judder of 26 mm is located in the middle of the aquifuge above the CECB mining panel and decreases up to its surrounding boundary, forming a typical subsidence basin. By contrast, the distribution of the tilt value is symmetrical with the perpendicular bisector of the *X* axis as the symmetrical point and the maximum values of 0.12 mm/m occur in the place of aquiclude over the two boundaries of the working face in the *X* direction, which is known as the open-off line and the stopping line. In addition, the maximum curvature of 0.0015 mm/m<sup>2</sup> arises in the water-resisting layer above the center of the mining panel, which is similar to the vertical displacement. The lowest value is situated in the vicinity of the working face. Hence, the curvature decreases to the minimum value of 0.0001 mm/m<sup>2</sup> first and then rises to 0.0009 mm/m<sup>2</sup> in the boundary of the model. Furthermore, the contour map of the horizontal displacement is similar to that of the tilt, with the maximum size of 6.5 mm at the overlying aquifuge over both sides of the CECB face along the *X* direction. The maximum horizontal deformation of 0.08 mm/m is in the center of the aquifuge, indicating the high probability of the development of vertical tensile fractures.

By using a similar method to the one above, the maximum values of the five deformation indexes of the water-resisting layer while using the CMFB with 55%, 65% and 85% fly ash were obtained, as shown in Figure 13.

The maximum values of five deformation indexes of the water-resisting layer decline first and then increase with the growing fly ash contents. When the fly ash proportion is 75%, the maximum value of all deformation indexes of the aquifuge is the smallest. The CMFB with 55% fly ash contributes to the five largest deformation indicators, which is completely opposite to the traditional cemented filling material using fly ash as aggregate and suggests that CO<sub>2</sub> and silicate additives exert a significant impact on the strength of the CMFB.

In a previous study on water preservation coal mining in the Yu-Shen mining area, the authors found that the index of horizontal deformation has a vital influence on the stability and integrity of the water-resisting layer. If the maximum horizontal deformation value of the aquifuge (red clay) exceeds 0.20 mm/m, which is greater than its allowable ultimate tensile strain, a vertical tensile micro-fracture in the aquiclude may occur. The micro-fractures are prone to developing into macro-cracks with wide aperture and high penetration rate under the condition of larger horizontal deformation. If the fractures go through the entire aquifuge and trigger a failure to resist water flow, the shallow water will percolate and flow into the mined-out area along the water-conducting fractures and water inrush will happen in the coal mine.

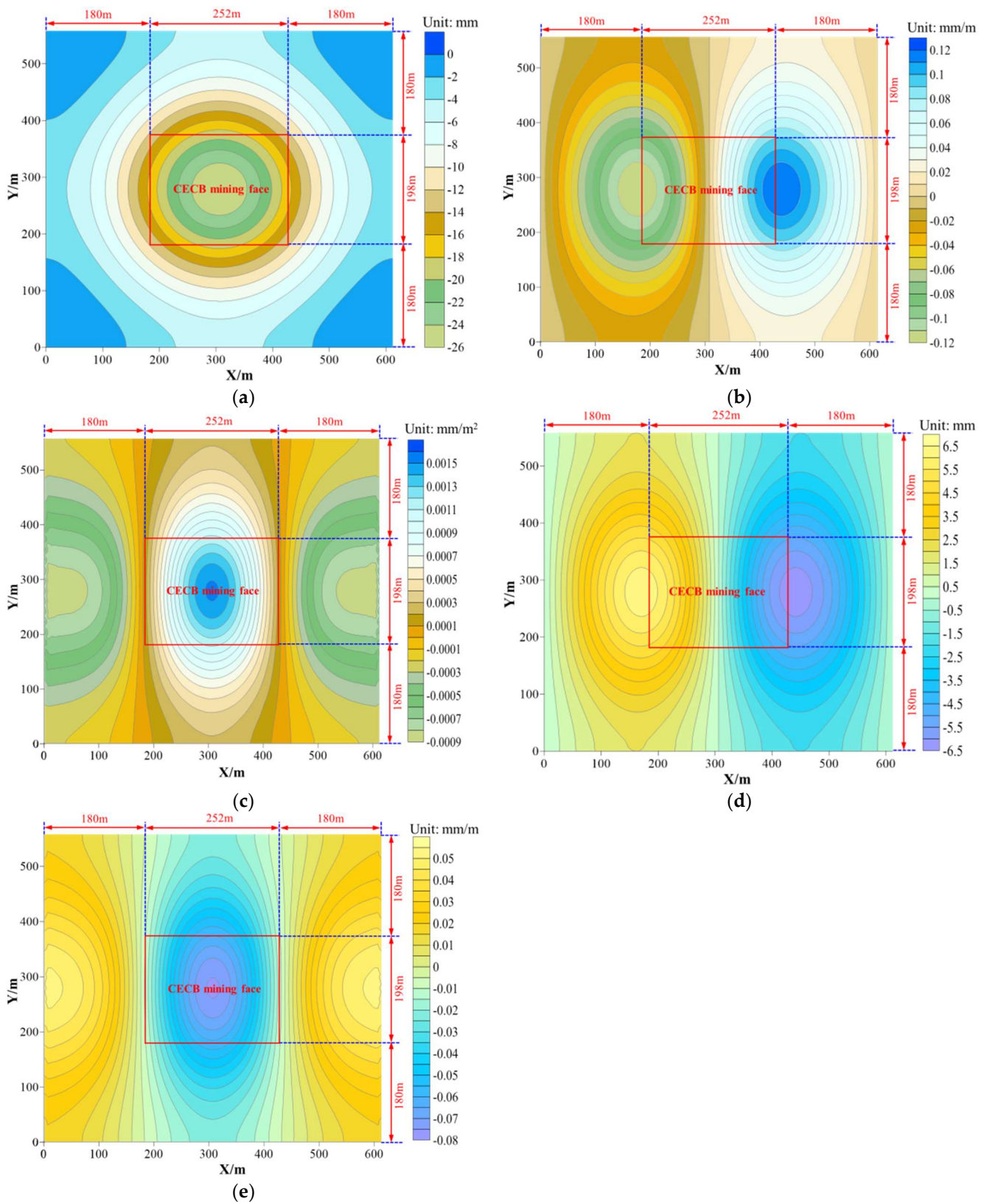


**Figure 12.** Numerical simulation results of the movement of aquifuge while using CECB and CMFB with 75% fly ash. (a) Vertical displacement; (b) tilt; (c) curvature; (d) horizontal displacement; (e) horizontal deformation.

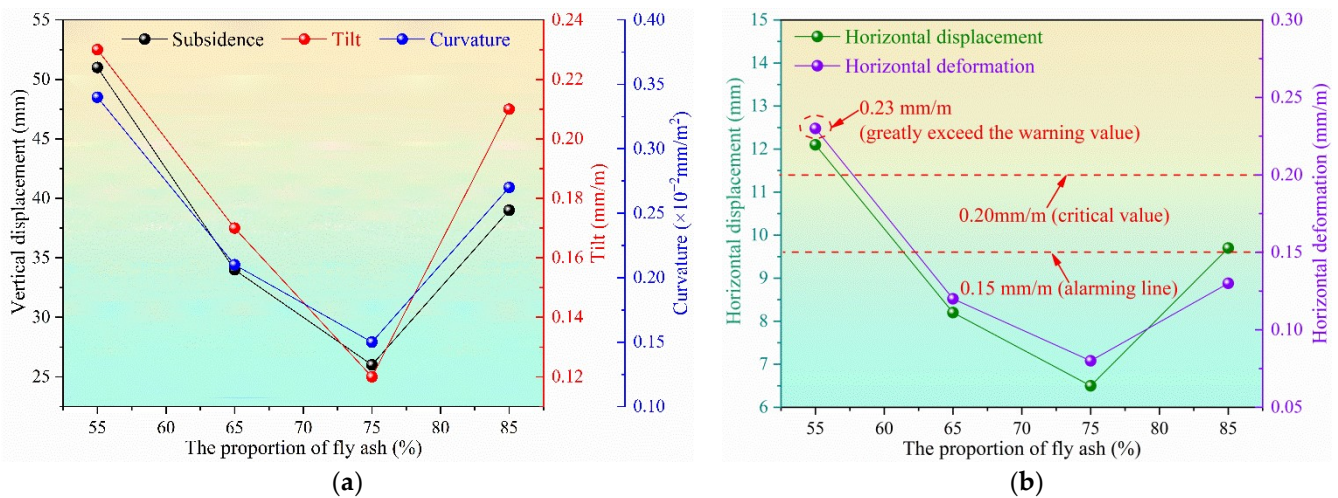


**Figure 13.** Numerical simulation results of the maximum values of five deformation indexes of the aquifuge with various proportions of fly ash. (a) The vertical displacement, tilt and curvature; (b) the horizontal displacement and horizontal displacement.

It can be seen from Figure 12b that the maximum horizontal deformation of the water-resisting layer is 0.23 mm/m while using CMFB with 55% fly ash content, which exceeds the critical value for realizing water-conserving coal mining. Moreover, the maximum horizontal deformation value corresponding to CMFB with 65% and 85% fly ash is 0.12 and 0.13 mm/m, both of which are approaching the warning value of 0.15 mm/m, and due consideration should thus be taken during the process of field implementation of CMFB.

#### 5.4. Water Table Lowering of the Shallow Water

##### 5.4.1. Establishment of Fluid–Solid Coupling Numerical Model

The fluid–solid coupling module was set to simulate the water level fluctuation of the shallow water while using CECB mining and CMFB with different fly ash contents. The “CONGIG fluid” code was employed to enter the seepage mode, and the “Initial PP” code was utilized to set the pore pressure and pore water pressure gradient. Moreover, the fluid–solid coupling numerical calculation mode was isotropic. The permeability coefficient of red clay (aquifuge) is less than  $10^{-7}$  cm/s. The permeability coefficients of hard rocks, i.e., mudstone, bauxitic mudstone, sandy mudstone, sandstone, fine sandstone, medium sandstone and limestone, are greater than that of red clay, and are listed in Table 5. The tensile strength of the fluid is set to  $10^{15}$  Pa and its porosity is set to 0.5, both of which are default values in the FLAC<sup>3D</sup> software. The saturation is set to 1 and the Biot coefficient is also set to 1. The “Fix pp” code was used to set the top surface loess (shallow water) as a free surface where the water can flow in or out, while the surrounding and bottom boundaries of the numerical simulation model were set as impermeable boundaries without penetrating fluids.

**Table 5.** The permeability coefficient of the overlying strata.

Number	Lithology	Permeability Coefficient (cm/s)
1	Red clay	$10^{-7}$
2	Mudstone	$10^{-6}$
3	Bauxitic mudstone	$10^{-5}$
4	Sandy mudstone	$10^{-5}$
5	Sandstone	$10^{-4}$
6	Fine sandstone	$10^{-4}$
7	Medium sandstone	$10^{-4}$
8	Limestone	$10^{-3}$

#### 5.4.2. Characteristics of Underground Aquifer in the Yu-Shen Coal Area

From bottom to top, there are total four types of aquifer in the Yu-Shen mining area, namely, the porous bedrock confined aquifer, burnt rock phreatic aquifer, Salawusu phreatic aquifer and unconsolidated porous phreatic aquifer, as shown in Figure 14.

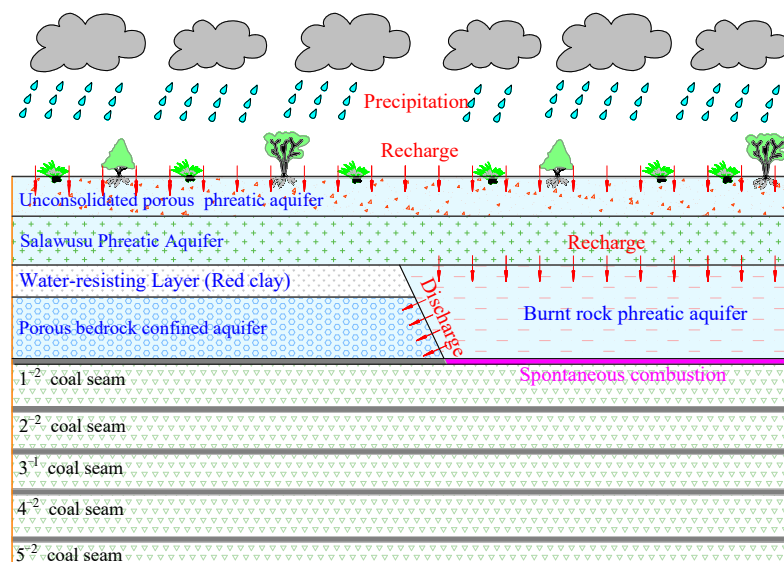


**Figure 14.** The major types of aquifers in Yu-Shen mining area.

The porous bedrock confined aquifer features minor porosity, high permeability, extremely low water yield property and restricted distribution range. Additionally, the burnt rock phreatic aquifer is primarily recharged from the overlying Salawusu phreatic aquifer and itself cannot form an independent water-storing formation. By contrast, the Salawusu Formation aquifer is widely distributed in the mining area, with thickness ranging from 0 m to 67.3 m and the water table being generally less than 10 m. The unconsolidated porous phreatic aquifer in the study area is weak and mainly recharged by precipitation, usually forming a united aquifer with the underlying Salawusu formation aquifer. The united buried shallow aquifer is what we called shallow water. It is the major aquifer in this area for domestic and ecological water supply, which needs to be considered during water conservation coal mining.

#### 5.4.3. Numerical Simulation Results of Water Table Lowering of Shallow Water

The water level fluctuation can be investigated according to the change in pore water pressure since the shallow water is not a confined aquifer. The groundwater depression cone and the contour map of water table lowering employing the CECB water-conserving coal mining method and CMFB with 75% fly ash are shown in Figure 15. The groundwater level has decreased by 0.47 m, indicating a narrow variation in groundwater level. In addition, the water level drop of the shallow aquifer using CMFB with different fly ash contents is shown in Figure 16.

The main types of vegetation in the study area are *Salix psammophila*, *Artemisia annua*, *Populus euphratica* and *Saliz matsudana*. The buried depth of shallow water ranges from 0.5 m to 1.8 m, and the surface vegetation is flourishing and exuberant. According to the field investigation of academician Wang Shuangming [30], the relationships between the growth conditions of the aforementioned vegetation and the shallow water level are listed in Table 6. It can be seen that when the buried depth of groundwater exceeds 3.0 m, the growth of surface vegetation will be restrained and thus degraded. Therefore, the water table drop should not be greater than the range varying from 1.2 m to 2.5 m. In order to ensure the flourishing growth of surface vegetation above the CECB mining face, the mining-induced water table lowering should be strictly less than 1.2 m.

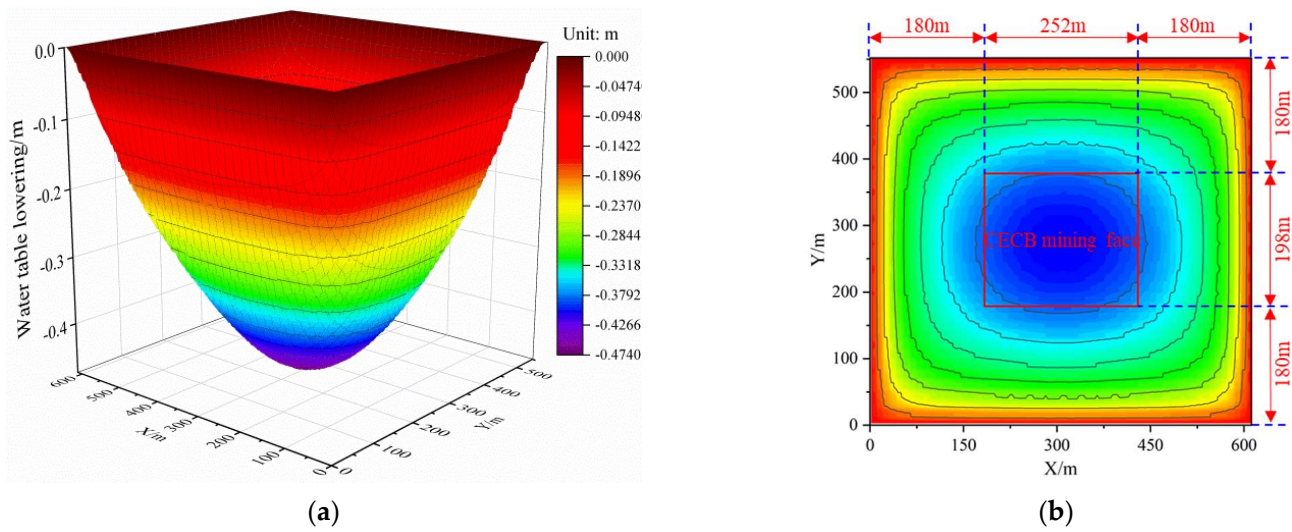


**Figure 15.** The numerical simulation results of shallow water level drop of the colliery when injecting the CMFB with 75% fly ash into the mined-out area. (a) The groundwater depression cone; (b) the contour map of water table lowering.

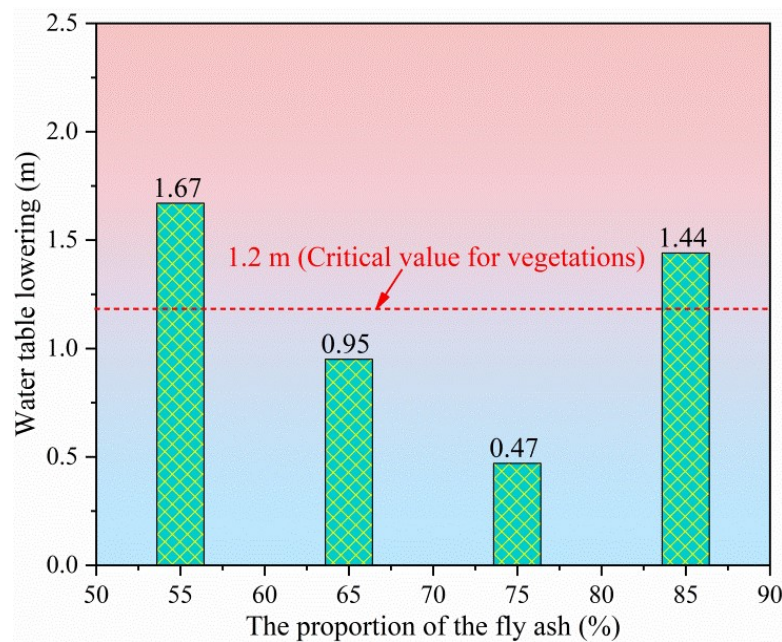


**Figure 16.** Fluid–mechanism coupling simulation of shallow water level lowering while injecting CMFB with different proportions of fly ash.

**Table 6.** The statistical results of the relationship between the growth of surface vegetation and the groundwater level [30].

Vegetation Type	Depth of the Shallow Buried Aquifer and the Growth of Vegetation			
Salix psammophila	<1.5 m (Luxuriant)	1.5 m–3.0 m (Good)	3.0 m–5.0 m (Normal)	>5.0 m (Poor)
Artemisia annua	<1.5 m (Luxuriant)	1.5 m–3.0 m (Good)	3.0 m–5.0 m (Normal)	>5.0 m (Poor)
Populus euphratica	<1.5 m (Luxuriant)	1.5 m–3.0 m (Good)	3.0 m–5.0 m (Normal)	>5.0 m (Poor)
Salix matsudana	<3.0 m (Luxuriant)	3.0 m–7.0 m (Good)	7.0 m–12.0 m (Normal)	>12.0 m (Poor)

According to Figure 16, the decline in water level using CMFB with 55% and 85% fly ash is 1.67 and 1.44 m, respectively, neither of which meet the requirements for water conservation coal mining. By contrast, the CECB mining method using CMFB with 65%

fly ash has caused a 0.95 m water table drop, 80% of the critical groundwater level drop for surface vegetation, and is therefore an alternative since it is under the threshold. It is apparent that the CMFB with 75% fly ash was the most suitable one to protect precious shallow water and surface vegetation, contributing to water and ecology preservation coal mining.

## 6. Discussion

This paper describes a prospective investigation on developing carbon dioxide mineralized filling body (CMFB) at ambient temperature and pressure and sequestering it in the MRs of the CECB mining method, offering a novel way to realize CO<sub>2</sub> sequestration. Additionally, CMFB development by using fly ash, etc. can contribute to the harmless treatment of solid wastes and prevent their pollution of air, soil and shallow water. Moreover, fly ash is cheap and can be widely obtained. Hence, selecting fly ash as aggregate in CMFB can greatly reduce the amount of cement and reduce the total filling costs. The research results are conducive to the coordinated development of coal extraction and water resource preservation, contributing to shifting the single situation of “water conservation mining” to “low-carbon collaborating solid waste treatment water conservation mining”. The paper provides a theoretical basis and reference for the field implementation of CMFB in the future and thus facilitates the construction of green and sustainable mining areas.

Traditional CO<sub>2</sub> mineralized coal-based solid waste technology needs catalytic nucleation at high temperature and pressure to improve the reaction rate of CO<sub>2</sub> and mineralized nodule rate, which is difficult to realize in large-scale industrialization. Therefore, it is of great scientific and engineering significance to explore and develop CO<sub>2</sub> coal-based solid waste filling materials at ambient temperature and pressure. On the other hand, it is necessary for the CO<sub>2</sub> mineralization process to be carried out continuously in a relatively confined space, which is coincident with the characteristics of the CECB mining method. The MR of CECB has good leak tightness during and after mining and filling, and the dimensions of the MR can be adjusted flexibly. By optimizing the layout and the dimensions of the MR, it can not only ensure the long-term mineralization of coal-based solid waste with CO<sub>2</sub>, but can also realize water preservation coal mining. However, the field application of CMFB needs to solve a series of problems, including large-scale CO<sub>2</sub> capture, filling material transportation and the weakening of the stability of CMFB after reacting with water.

At present, water preservation mining methods are primarily harmonic mining, partial mining, curtain grouting, overburden bed separation grouting and backfill mining. Harmonic mining optimizes the working face layout, the mining sequence and the advancing direction uniformly to counteract the movement of overlying strata. However, its popularity and applicability are limited due to the various distributions of protected objects (overlying aquifers, buildings and structures). In addition, the partial mining left coal pillar unmined permanently or abandon a portion of coal resources to support the roof and thus realize the mitigation of overburden deformation and thus shallow water loss. Hence, large amounts of resources are wasted and there is a low recovery rate of generally less than 50%. Additionally, curtain grouting injects the slurry into the cracks, pores or mining-induced fractures between the overlying shallow water and the mined-out area. The purpose of the method is to form a continuous curtain that can block the water percolation channel from the overlying aquifer to the gob. However, it suffers from limited adaptability and curtain instability after grouting in the long term. The overburden separation grouting fills the stratum separation space by drilling grouting, so as to mitigate the overburden subsidence and thus preserve the shallow aquifer. It can only be applied in the bed separation space where the lithology of the upper stratum is harder than that of the lower and the effects of reducing overburden subsidence are restricted. Backfill mining is currently the most effective method to control overlying layer migration and thus conserve the shallow water since it substitutes the coal body with the filling body to support the roof of the mined-out area, which can significantly lighten the overlying layer migration and shallow water loss [6].

Backfill mining is primarily longwall backfill mining and shortwall backfill mining. The former has the problems of insufficient filling time and filling space. The roof of the mined-out area subsides and collapses immediately after the coal seam is extracted. However, it takes a long time for the backfill to reach its designed strength, and the goaf roof cannot be supported in time. Therefore, the movement of the overlying strata is inevitable, giving rise to difficulty in safe and high-efficient coal extraction under shallow water. Moreover, since the mining and filling exist in the same space and are not separated completely in longwall backfill mining, the filling speed affects extraction progress, while equipment maintenance delays the filling process, contributing to the mutual influence and restriction between extraction and backfill. It is arduous for them to operate in parallel. By contrast, the CECB mining method sets the coal extraction roadway and the backfill roadway in two different positions, with a large distance between them. Skip and interval mining offer a separated space for extraction and backfill which ensures isolated filling and mining processes and can realize mining and filling simultaneously without mutual restrictions and effects. Additionally, the width of the roadway is narrow compared with that of longwall backfill mining which can reduce the immediate roof subsidence effectively [7].

The CECB method has the advantages of integrating extraction and excavation, parallel mining and filling operation, convenient moving of the working face, low investment and high recovery rate over other mining methods. Compared with traditional longwall backfill mining, the CECB method arranges the coal extraction system and backfill system in different positions, avoiding the interaction between mining and filling operation, and thus the working efficiency can be ensured. The exposed area of each MR is small and results in limited subsidence of the roof before backfill, which is beneficial to the primary stability of CMFB before reaching the designed strength. Therefore, CMFB is an ideal backfill material for CECB. However, the feasibility of other backfill mining methods, such as longwall backfill mining, needs further study, due to the fact that their mining processes are essentially different from that of CECB mining. For example, the mining space of longwall backfill mining is not completely separated from the filling space. It seems that injecting the CMFB into the flexible bags set ahead in the filling space is the only option, which may lead to CMFB instability since it cannot be sealed due to the rupture of the flexible materials.

The authors developed high water swelling filling material with fly ash as aggregate and lime, anhydrite, cement and additives as ingredients [8]. The viscosity, bleeding rate, expansion rate, uniaxial compressive strength, slump, initial setting and final setting time of specimens with different water–solid ratios were studied. With due consideration given to the specific engineering and geological conditions of the colliery, the reasonable water–solid ratio and the material ratio of filling materials were determined. In the XV2309 working face of Wangtaipu Coal Mine in Shanxi Province, an industrial test was carried out with the developed filling material [39]. The strength of the filling body is 5 MPa with 60 days' setting time, the average expansion rate is 7.63% and the average bleeding rate is only 0.1%. The deformation of the water-resisting layer is mitigated and water table lowering of the overlying aquifer is effectively controlled and reduced. The filling cost per ton of coal when all MRs are backfilled is CNY 120, which is slightly higher than CNY 100 for longwall backfill mining. In addition, the maximum daily and annual output of CECB exceeds 3000 t and 600,000 t, respectively, almost the same as that of longwall backfill mining. The previous research on the CECB mining method and the development and field application of high water expansion filling materials laid a solid foundation for further study on the field implementation of CMFB in future.

In general, the CECB water preservation mining method meets the strategic requirements of the coordinated development of coal resources and the ecological environment. It has been popularized and applied to Yuxing Colliery, Wangtaipu Colliery, Suncun Colliery, etc. in northwest China, since it can make full harmless use of solid wastes accumulated around the mining areas on the premise of safe and highly efficient coal extraction with a

high recovery rate. The practice results show that good economic, social and environmental benefits have been achieved in the aforementioned collieries. According to statistics, as of the end of 2020, a total of 2.60 million tons of coal resources have been recovered by CECB in dozens of coal mines and a total new profit of more than 40 million dollars has been achieved [11]. However, all the previous field implementations of CECB used cement paste filling materials, crushed gangue or high water content filling materials. At present, the field application of CO<sub>2</sub> gas adhering to the filling materials to realize CO<sub>2</sub> sequestration has not been reported. In following research, a scanning electron microscope, X-ray diffraction, Vicat instrument, etc. will be employed to analyze the mesostructure, setting time and the rheological properties of the CMFB, and further exploration of the mechanism of the reaction among CO<sub>2</sub> gas, solid wastes and additives will be carried out, so as to provide a valuable theoretical research basis for the field implementations of CMFB in the future.

In view of the hydrogeological conditions where the distance between the overlying aquifer and the coal seam is large and the aquiclude between them is thick, the material ratios of filling materials can be adjusted to cut down the filling cost on the premise of mitigating the overburden migration and thus preserving water resources. For example, in the industrial test of Wangtaipu Coal Mine, we adjusted the water–solid ratio of the filling body in the last mining phase from 0.8:1 to 0.9:1 since the water level is controlled successfully in the early mining phase. In addition, further study on the deformation of the aquiclude and the fluctuation of the water level under the conditions of partial backfill of MRs in CECB will be conducted. If the shallow water preservation coal mining can be realized without filling in the last one or two mining phases, a further reduction in filling cost will become reality.

## 7. Conclusions

The conclusions drawn from the research are as follows:

(1) The scientific concept of developing CMFB by making CO<sub>2</sub> react with coal-based solid waste such as fly ash at a normal temperature and pressure and injecting it into the confined MR of the CECB mining method, was proposed. It can contribute to constructing the “trinity” of green and low-carbon mining areas, with permanent CO<sub>2</sub> storage, harmless treatment of coal-based solid wastes and shallow water preservation.

(2) The CMFB was developed at ambient temperature and pressure by using fly ash as aggregate, and CO<sub>2</sub> gas, silicate additives and cement as accessories. The UCS and tensile strength of CMFB with various curing times (3 d, 7 d, 14 d, 28 d) and different fly ash contents (55%, 65%, 75%, 85%) were tested indoors. The test results show that the compressive and tensile strength of CMFB increases with longer setting time. With the rising fly ash proportion, the compressive strength of CMFB increases first and then decreases, reaching the maximum when the fly ash content is 75%, while the tensile strength diminishes continuously.

(3) The commonly and extensively utilized filling materials are primarily cemented filling materials, crushed gangue and high water content filling materials. When the backfill mining method was previously employed to extract coal bodies beneath the overlying aquifer on the premise of water preservation and conservation, measures were usually adjusted to local conditions and the filling bodies were developed by taking materials from a wide range of sources as the raw materials. For instance, in view of the typical geological feature of aeolian sand, widely distributed in the Yu-Shen mining area, Shaanxi province, northwest China, Liu Pengliang et al. developed a new aeolian sand paste-like material with aeolian sand being used as aggregate and alkali-activated fly ash being utilized as a cementing agent. It was then applied to the Yuyang Colliery and the problem of damage to Salawusu Formation Aquifer caused by longwall caving mining was tackled [53]. Additionally, in view of the collieries without sufficient and abundant gangue accumulation, Zhou Nan et al. developed a sand-based cemented paste filling material with widely distributed and low-cost Yellow River sand as filling aggregate and cement and fly ash as binder for Zhaoguan Colliery in Shandong Province of China, which is only 5 km away from

the Yellow River [48]. Zhou Huaqiang et al. used the developed paste filling materials to extract a large number of coal resources under the village [54]. Feng Guangming developed ultra-high water filling material and put forward the corresponding mining technology [55]. However, the above mining methods and filling materials only take the harmless treatment of solid wastes and the overlying aquifer preservation into account, without regarding CO<sub>2</sub> sequestration as one of the purposes of backfill mining. This paper brings the large-scale treatment of CO<sub>2</sub> into the scientific framework of colliery green mining, and puts forward the trinity concept of green mining for CO<sub>2</sub> sequestration, harmless treatment of solid wastes and shallow water table preservation, which is innovative compared with the previous research on water conservation coal mining. The research results can provide theoretical guidance for the development and field application of CMFB, and promote construction of green, low-carbon and sustainable coal areas.

(4) According to the stress–strain curve of the CMFB from the indoor UCS test, the material ratio of the similar material of CMFB was optimized and determined. The physical analogue model was then constructed to simulate the mining-induced deformation of the overburden and aquifuge while using the CECB mining. The subsidence of the aquiclude from physical analogue simulation shows good agreement with that from the numerical simulation. The maximum vertical displacement of the water-resisting layer is 28 m, only 7.7% higher than that of the numerical simulation.

(5) The FLAC<sup>3D</sup> finite element software was employed to simulate the aquifuge deformation and water table lowering. The CMFB with 14 d curing time and various fly ash contents were taken for analysis. Based on the indoor test results and the numerical simulation results, the strain-softening parameters of CMFB in the numerical simulation model were calibrated systematically. The deformation of the water-resisting layer and the decline in the water level of the shallow water while injecting CMFB with different fly ash contents into the MRs of CECB were obtained. The CMFB with 75% fly ash can effectively protect the integrity and water-blocking stability of the overlying aquiclude and mitigate the water level drop of the underground aquifer, thus preserving the shallow water and surface vegetation and contribute to the construction of green and sustainable ecological mines.

**Author Contributions:** Y.X. conceived the research and wrote the original draft. L.M. revised and reviewed the manuscript. I.N. contributed to formal analysis. J.Z. was responsible for data curation. All authors have read and agreed to the published version of the manuscript.

**Funding:** This paper was funded by the National Natural Science Foundation of China (51874280) and the Fundamental Research Funds for the Central Universities (2021ZDPY0211).

**Institutional Review Board Statement:** Not applicable.

**Informed Consent Statement:** Not applicable.

**Data Availability Statement:** Not applicable.

**Acknowledgments:** This work was supported by the Fundamental Research Funds for the Central Universities (2017XKQY096), and the Priority Academic Program Development of Jiangsu Higher Education Institutions (PAPD).

**Conflicts of Interest:** The authors declare that they have no competing financial interest in connection with the work submitted.

## Abbreviations

CECB	continuous extraction and continuous backfill
CMFB	carbon dioxide mineralized filling body
UCS	uniaxial compressive strength
MRs	mining roadways
FA	fly ash
CM	cement

FA55	the ratios of the fly ash to the total of the fly ash and the cement are 55%
FA65	the ratios of the fly ash to the total of the fly ash and the cement are 65%
FA75	the ratios of the fly ash to the total of the fly ash and the cement are 75%
FA85	the ratios of the fly ash to the total of the fly ash and the cement are 85%

## References

- Xu, Y.; Ma, L.; Khan, N.M. Prediction and maintenance of water resources carrying capacity in mining area—a case study in the yu-shen mining area. *Sustainability* **2020**, *12*, 7782. [\[CrossRef\]](#)
- Zhang, D.; Fan, G.; Ma, L.; Wang, X. Aquifer protection during longwall mining of shallow coal seams: A case study in the Shendong Coalfield of China. *Int. J. Coal. Geol.* **2011**, *86*, 190–196. [\[CrossRef\]](#)
- Li, L.; Li, F.; Zhang, Y.; Yang, D.; Liu, X. Formation mechanism and height calculation of the caved zone and water-conducting fracture zone in solid backfill mining. *Int. J. Coal Sci. Technol.* **2020**, *7*, 208–215. [\[CrossRef\]](#)
- Ma, L.; Jin, Z.; Liang, J.; Sun, H.; Zhang, D.; Li, P. Simulation of water resource loss in short-distance coal seams disturbed by repeated mining. *Environ. Earth Sci.* **2015**, *74*, 5653–5662. [\[CrossRef\]](#)
- Ma, L.; Zhang, D.; Jin, Z.; Wang, S.; Yu, Y. Theories and methods of efficiency water conservation mining in short-distance coal seams. *J. Chin. Coal Soc.* **2019**, *44*, 727–738.
- Xu, Y. Study on “Five Maps, Three Zones and Two Zoning Plans” Water Conservation Mining Method in Yu-Shen Mining Area. Master’s Thesis, China University of Mining Science & Technology, Xuzhou, China, 2019.
- Xu, Y.; Ma, L.; Yu, Y. Water preservation and conservation above coal mines using an innovative approach: A case study. *Energies* **2020**, *13*, 2818. [\[CrossRef\]](#)
- Wang, A.; Ma, L.; Wang, Z.; Zhang, D.; Li, K.; Zhang, Y.; Yi, X. Soil and water conservation in mining area based on ground surface subsidence control: Development of a high-water swelling material and its application in backfilling mining. *Environ. Earth Sci.* **2016**, *75*, 779. [\[CrossRef\]](#)
- Sun, K.; Fan, L.; Xia, Y.; Li, C.; Chen, J.; Gao, S.; Wu, B.; Peng, J.; Ji, Y. Impact of coal mining on groundwater of Luohe Formation in Binchang mining area. *Int. J. Coal Sci. Technol.* **2021**, *8*, 88–102. [\[CrossRef\]](#)
- Fan, L.; Ma, L.; Yu, Y.; Wang, S.; Xu, Y. Water-conserving mining influencing factors identification and weight determination in northwest China. *Int. J. Coal Sci. Technol.* **2019**, *6*, 95–101. [\[CrossRef\]](#)
- Fan, L.; Ma, X. A review on investigation of water-preserved coal mining in western China. *Int. J. Coal Sci. Technol.* **2018**, *5*, 411–416. [\[CrossRef\]](#)
- Newman, C.; Agioutantis, Z.; Leon, G.B.J. Assessment of potential impacts to surface and subsurface water bodies due to longwall mining. *Int. J. Min. Sci. Technol.* **2017**, *27*, 57–64. [\[CrossRef\]](#)
- Stoner, J.D. Probable hydrologic effects of subsurface mining. *Ground Water Monit. R.* **1983**, *3*, 128–137. [\[CrossRef\]](#)
- Karaman, A.; Akhiev, S.S.; Carpenter, P.J. A new method of analysis of water-level response to a moving boundary of a longwall mine. *Water Resour. Res.* **1999**, *35*, 1001–1010. [\[CrossRef\]](#)
- Shultz, R.A. *Ground-Water Hydrology of Marshall County, West Virginia, with Emphasis on the Effects of Longwall Coal Mining*, 3rd ed.; New York Press: New York, NY, USA, 1988; pp. 68–106.
- Booth, C.J.; Spande, E.D.; Pattee, C.T.; Miller, J.D.; Bertsch, L.P. Positive and negative impacts of longwall mine subsidence on a sandstone aquifer. *Environ. Earth Sci.* **1998**, *34*, 223–233. [\[CrossRef\]](#)
- Booth, C. Groundwater as an environmental constraint of longwall coal mining. *Environ. Earth Sci.* **2006**, *49*, 796–803. [\[CrossRef\]](#)
- Hill, J.G.; Price, D.R. The impact of deep mining on an overlying aquifer in western pennsylvania. *Ground Water Monit. R.* **1983**, *3*, 138–143. [\[CrossRef\]](#)
- Howladar, M.F.; Karim, M.M. The selection of backfill materials for Barapukuria underground coal mine, Dinajpur, Bangladesh: Insight from the assessments of engineering properties of some selective materials. *Environ. Earth Sci.* **2015**, *73*, 6153–6165. [\[CrossRef\]](#)
- Howladar, M.F. Coal mining impacts on water environs around the Barapukuria coal mining area, Dinajpur, Bangladesh. *Environ. Earth Sci.* **2012**, *70*, 215–226. [\[CrossRef\]](#)
- Gandhe, A.; Venkateswarlu, V.; Gupta, R.N. Extraction of coal under a surface water body—A strata control investigation. *Rock Mech. Rock Eng.* **2005**, *38*, 399–410. [\[CrossRef\]](#)
- Kim, J.M.; Parizek, R.R.; Elsworth, D. Evaluation of fully-coupled strata de-strata and groundwater flow in response to longwall mining. *Int. J. Rock Mech. Min. Sci.* **1997**, *34*, 1187–1199. [\[CrossRef\]](#)
- Raghavendra, N.S.; Deka, P.C. Sustainable development and management of ground water resources in mining affected area: A review. *Procedia Earth Planet. Sci.* **2015**, *11*, 598–604. [\[CrossRef\]](#)
- Tiwary, R.K. Environmental impact of coal mining on water regime and its management. *Water Air Soil Pollut.* **2001**, *132*, 185–199. [\[CrossRef\]](#)
- Robertson, J. Challenges in sustainably managing groundwater in the Australian Great Artesian Basin: Lessons from current and historic legislative regimes. *Hydrogeol. J.* **2020**, *28*, 343–360. [\[CrossRef\]](#)
- Fan, L. Scientific connotation of water-preserved mining. *J. Chin. Coal Soc.* **2017**, *42*, 27–35.
- Huang, Q. Impermeability of overburden rock shallow buried coal seam and classification of water conservation mining. *Chin. J. Rock Mech. Eng.* **2010**, *29*, 3622–3627.

28. Huang, Q. Simulation of clay aquiclude stability of water conservation mining in shallow-buried coal seam. *Chin. J. Rock Mech. Eng.* **2009**, *28*, 987–992.
29. Wang, S.; Huang, Q.; Fan, L.; Yang, Z.; Shen, T. Study on overburden aquiclude and water protection mining regionization in the ecological fragile mining area. *J. Chin. Coal Soc.* **2010**, *35*, 7–14.
30. Wang, S.; Huang, Q. *Coal Mining and Ecological Water Level Protection in Ecologically Fragile Areas*, 3rd ed.; Science Press: Beijing, China, 2010; pp. 92–106.
31. Wang, X.; Qin, D.; Zhang, D.; Sun, C.; Zhang, C.; Xu, M.; Li, B. Mechanical characteristics of superhigh-water content material concretion and its application in longwall backfilling. *Energies* **2017**, *10*, 1592. [[CrossRef](#)]
32. Wang, S.; Ma, L. Characteristics and control of mining induced fractures above longwall mines using backfilling. *Energies* **2019**, *12*, 4604. [[CrossRef](#)]
33. Huang, Y.; Zhang, J.; Yin, W.; Sun, Q. Analysis of overlying strata movement and behaviors in caving and solid backfilling mixed coal mining. *Energies* **2017**, *10*, 1057. [[CrossRef](#)]
34. Zhang, J.; Zhang, Q.; Sun, Q.; Gao, R.; Germain, D.; Abro, S. Surface subsidence control theory and application to backfill coal mining technology. *Environ. Earth Sci.* **2015**, *72*, 1439–1448. [[CrossRef](#)]
35. Ma, L.; Zhang, D.; Wang, S.; Xie, Y.; Yu, Y. Water-preserved mining with the method named “backfilling while mining”. *J. Chin. Coal Soc.* **2018**, *43*, 62–69.
36. Zhang, J.X.; Sun, Q.; Zhou, N.; Jiang, H.Q. Research and application of roadway backfill coal mining technology in western coal mining area. *Arab. J. Geosci.* **2016**, *9*, 558. [[CrossRef](#)]
37. Cao, Z.Z. Joint bearing mechanism of coal pillar and backfilling body in roadway backfilling mining technology. *CMC-Comput. Mater. Con.* **2018**, *54*, 137–159.
38. Ma, L.; Xu, Y.; Zhang, D.S.; Lai, X.; Huang, K.; Du, H. Characteristics of aquiclude and surface deformation in continuous mining and filling with wall system for water conservation. *J. Min. Saf. Eng.* **2019**, *36*, 30–36.
39. Ma, L.; Jin, Z.; Liu, W.; Zhang, D.; Zhang, Y. Wongawilli roadway backfilling coal mining method—A case study in Wangtaipu coal mine. *Int. J. Oil Gas Coal Technol.* **2019**, *20*, 342–359. [[CrossRef](#)]
40. Yu, Y.; Ma, L. Application of roadway backfill mining in water-conservation coal mining: A case study in Northern Shaanxi, China. *Sustainability* **2019**, *11*, 3719. [[CrossRef](#)]
41. Yu, Y.; Ma, L.; Zhang, D. Characteristics of roof ground subsidence while applying a continuous excavation continuous backfill method in longwall mining. *Energies* **2020**, *13*, 95. [[CrossRef](#)]
42. Brent, G.F.; Allen, D.J.; Eichler, B.R.; Petrie, J.G.; Mann, J.P.; Haynes, B.S. Mineral carbonation as the core of an industrial symbiosis for energy-intensive minerals conversion. *J. Ind. Ecol.* **2012**, *16*, 94–104. [[CrossRef](#)]
43. Uliasz, B.A.; Mokrzycki, E. The potential of FBC fly ashes to reduce CO<sub>2</sub> emissions. *Sci. Rep.* **2020**, *10*, 1–9.
44. Olajire, A.A. A review of mineral carbonation technology in sequestration of CO<sub>2</sub>. *J. Petrol. Sci. Eng.* **2013**, *109*, 364–392. [[CrossRef](#)]
45. Lippiatt, N.; Ling, T.C.; Pan, S.Y. Towards carbon-neutral construction materials: Carbonation of cement-based materials and the future perspective. *J. Build. Eng.* **2020**, *28*, 101062. [[CrossRef](#)]
46. Morandeau, A.; Thiéry, M.; Dangla, P. Impact of accelerated carbonation on OPC cement paste blended with fly ash. *Cem. Concr. Res.* **2015**, *67*, 226–236. [[CrossRef](#)]
47. Moon, E.J.; Choi, Y.C. Carbon dioxide fixation via accelerated carbonation of cement-based materials: Potential for construction materials applications. *Constr. Build. Mater.* **2019**, *199*, 676–687. [[CrossRef](#)]
48. Zhou, N.; Zhang, J.; Ouyang, S.; Deng, X.; Dong, C.; Du, E. Feasibility study and performance optimization of sand-based cemented paste backfill materials. *J. Clean. Prod.* **2020**, *259*, 120798. [[CrossRef](#)]
49. Wang, G.; Xu, Y.; Ren, H. Intelligent and ecological coal mining as well as clean utilization technology in China: Review and prospects. *Int. J. Min. Sci. Technol.* **2019**, *29*, 161–169. [[CrossRef](#)]
50. Qi, C.; Fourie, A. Cemented paste backfill for mineral tailings management: Review and future perspectives. *Miner. Eng.* **2019**, *144*, 106025. [[CrossRef](#)]
51. Belem, T.; Benzaazoua, M. Design and application of underground mine paste backfill technology. *Geotech. Geol. Eng.* **2008**, *26*, 147–174. [[CrossRef](#)]
52. Luo, Y.; Wu, Y.; Ma, S.; Zheng, S.; Zhang, Y.; Chu, P.K. Utilization of coal fly ash in China: A mini-review on challenges and future directions. *Environ. Sci. Pollut. Res.* **2021**, *28*, 18727–18740. [[CrossRef](#)]
53. Liu, P.; Zhang, H.; Cui, F.; Sun, K.; Sun, W. Technology and practice of mechanized backfill mining for water protection with aeolian sand paste-like. *J. Chin. Coal Soc.* **2017**, *42*, 118–126.
54. Chang, Q.; Yuan, C.; Wang, Y.; Zhang, B.; Zhou, H.Q. Semi-convex mechanical analysis on stability of step coal wall in fully mechanized mining with paste filling. *J. Chin. Univ. Min. Technol.* **2022**, *51*, 46–55.
55. Feng, G.; Wang, C.; Li, F.; Jia, K. Research on bag-type filling mining with super-high-water material. *J. Min. Saf. Eng.* **2011**, *28*, 602–607.